Meteorologically-Informed Spatial Planning of European PV Deployment to Reduce Multiday Generation Variability

Mühlemann, Dirk; Folini, Doris; Pfenninger, Stefan; Wild, Martin; Wohland, Jan

DOI
10.1029/2022EF002673

Publication date
2022

Document Version
Final published version

Published in
Earth's Future

Citation (APA)
Mühlemann, D., Folini, D., Pfenninger, S., Wild, M., & Wohland, J. (2022). Meteorologically-Informed Spatial Planning of European PV Deployment to Reduce Multiday Generation Variability. *Earth's Future*, *10*(7), Article e2022EF002673. https://doi.org/10.1029/2022EF002673

Important note
To cite this publication, please use the final published version (if applicable).
Please check the document version above.

Earth's Future

RESEARCH ARTICLE
10.1029/2022EF002673

Meteorologically-Informed Spatial Planning of European PV Deployment to Reduce Multiday Generation Variability

Dirk Mühlemann[1], Doris Folini[1], Stefan Pfenninger[2], Martin Wild[1], and Jan Wohland[3,4]

[1]Institute for Atmospheric and Climate Science, ETH Zurich, Zürich, Switzerland, [2]Faculty of Technology, Policy and Management (TPM), Delft University of Technology, Delft, The Netherlands, [3]Institute for Environmental Decisions, ETH Zurich, Zürich, Switzerland, [4]Now at Climate Service Center Germany (GERICS), Helmholtz-Zentrum Hereon, Hamburg, Germany

Key Points:

- Year-round weather regime classification with linked photovoltaic (PV) capacity factors per country in Europe
- European multiday PV variability could be as high as 43.8 GW in 2050
- Optimized distribution of PV systems in Europe reduces multiday variability up to 40%

Supporting Information:

Supporting Information may be found in the online version of this article.

Correspondence to:

D. Mühlemann,
dirk.muehlemann@usys.ethz.ch

Citation:

Mühlemann, D., Folini, D., Pfenninger, S., Wild, M., & Wohland, J. (2022). Meteorologically-informed spatial planning of European PV deployment to reduce multiday generation variability. *Earth's Future*, *10*, e2022EF002673. https://doi.org/10.1029/2022EF002673

Received 14 JAN 2022
Accepted 22 JUN 2022

Author Contributions:

Conceptualization: Dirk Mühlemann, Doris Folini, Stefan Pfenninger, Martin Wild, Jan Wohland
Data curation: Dirk Mühlemann
Formal analysis: Dirk Mühlemann
Investigation: Dirk Mühlemann
Methodology: Dirk Mühlemann, Doris Folini, Stefan Pfenninger, Jan Wohland
Project Administration: Jan Wohland
Software: Dirk Mühlemann
Supervision: Doris Folini, Stefan Pfenninger, Martin Wild, Jan Wohland
Validation: Dirk Mühlemann, Doris Folini, Stefan Pfenninger, Martin Wild, Jan Wohland
Visualization: Dirk Mühlemann

Abstract Renewable generation variability over multiple days is a key challenge in decarbonizing the European power system. Weather regimes are one way to quantify this variability, but so far, their applications to energy research have focused on wind power generation in winter. However, the projected growth of solar photovoltaic (PV) capacity implies that its absolute variability across the continent will grow substantially. Here we combine weather regimes based on ERA5 reanalysis data with country-specific capacity factors to investigate multiday PV generation variability in Europe. With current installed capacity (131 GW), total PV production in Europe (52.3 GW) varies by 0.9 GW on average, with a maximum change of 3.0 GW, upon transition from one weather regime to another. Using projected PV capacity for 2050 (1.94 TW), variability would rise to 13.9 and 43.8 GW. We present optimized spatial distributions of capacity additions in three scenarios that substantially reduce variability by up to 40%. One of them ascertains a large local PV production, thereby minimizing the need for long-range power transmission while still reducing variability by about 30%, highlighting that optimized siting and local generation can be reconciled. Our results emphasize the value of leveraging climate information in decarbonizing power systems.

1. Introduction

Photovoltaic (PV) power production will likely become a central pillar of renewable power generation in Europe in the future. Its power generation depends on weather conditions, especially surface solar radiation (Huld et al., 2010), and is thus subject to significant fluctuations, including at the time scale of days to weeks, where longer-lasting large-scale patterns called weather regimes dominate weather at the continental scale (Drücke et al., 2020; Graabak & Korpås, 2016; Stram, 2016).

To operate a stable power grid, electricity production must always equal consumption. Mismatches between production and consumption cause deviations from the desired grid frequency and can cause damage to connected electrical devices and power outages (Machowski et al., 2020). The increasing reliance on weather-dependent renewables, namely wind and PV, requires accurate estimates of renewable generation variability to balance the power grid. Transmission infrastructure in combination with informed siting of generators allows to significantly reduce the variability of renewables because below-average PV production in one region may be buffered by an above-average production elsewhere (Rasmussen et al., 2012). Such benefits of spatial smoothing can be understood based on weather regimes. But a systematic application of weather regimes to understand the year-round multiday variability of PV power generation is currently missing in the literature. Multiday lulls compromise reliable energy supply because they can not be bridged with batteries and instead depend on long-duration storage possibilities, dispatchable backup capacity or demand-side flexibility, making investigation of them of great interest.

While different approaches exist, weather regimes are typically based on empirical orthogonal function (EOF) analysis and k-mean clustering of geopotential height in winter (Cassou, 2008; Michelangeli et al., 1995). Geopotential height denotes the height at which atmospheric pressure drops to a certain pressure level, for example, 500 hPa. This altitude is higher in high-pressure regions than in low-pressure regions. In Europe, large geopotential height thus tends to be associated with fair weather, whereas small geopotential height is rather indicative of stormy conditions. By combining weather regime classification with renewable generation and electricity consumption patterns, we can determine the stress for the energy system induced by weather regime conditions (Brayshaw et al., 2011; Ely et al., 2013; Grams et al., 2017; Jerez et al., 2013; van der Wiel et al., 2019). More

Writing – original draft: Dirk Mühlemann
Writing – review & editing: Dirk Mühlemann, Doris Folini, Stefan Pfenninger, Martin Wild, Jan Wohland

complex methods combine renewable generation with demand to derive "Targeted Circulation Types" focusing on a specific application case (Bloomfield et al., 2020).

So far, most European weather regime applications to energy research have focused on wind power generation in winter. Because in Europe, wind power currently dwarfs PV power generation in many locations in terms of total generation and variability amplitudes (Grams et al., 2017). Furthermore, electricity demand in Europe is highest in winter, increasing energy system stress and making the season particularly relevant for reliability assessments (van der Wiel et al., 2019). It has led to the four well-known weather regimes (positive and negative phase of the North Atlantic Oscillation, Scandinavian blocking, and Atlantic ridge) whose impact on the European energy system in winter is very well researched (Brayshaw et al., 2011; Ely et al., 2013; Grams et al., 2017; Jerez et al., 2013; van der Wiel et al., 2019).

Fewer studies have applied weather regimes to understand renewable power generation variability during an entire year (Grams et al., 2017). However, we need an in-depth understanding of variability during all seasons because renewables are expected to play a pivotal role in energy system decarbonization in the next decades. Following European (European Commission, 2019) and international policies (Schleussner et al., 2016), the future power system must operate reliably at all hours of the year while eliminating carbon emissions. In addition, seasons other than winter may become more important in the future. For instance, in the European summer, electricity demand is expected to increase in southern countries for cooling demand, increasing energy system stress in summer (Jakubcionis & Carlsson, 2017). A year-round analysis with possible future scenarios is crucial to fill this knowledge gap.

To our knowledge, only one study applies weather regimes to reduce renewable generation variability, finding that climate-informed spatial deployment of wind fleets can substantially reduce multiday European wind generation variability (Grams et al., 2017). While briefly mentioning PV generation variability, this study focused on wind power due to substantially higher current wind capacities. Therefore, a thorough assessment of PV using weather regimes is still missing even though PV panels are heavily deployed and may become the dominant electricity source globally. For instance, Manish Ram et al. (2017) estimate that installed 2050 PV capacity for a 100% renewable scenario in Europe must rise to 1.94 TW while the International Renewable Energy Agency (IRENA) estimate 0.89 TW (IRENA, 2020a). And according to others, these numbers may well be even higher (SolarPower Europe and LUT University, 2020). Although these estimates are based on model runs with particular assumptions, they indicate that a 10-fold to 20-fold increase of installed PV capacity is needed, implying that the impact of multiday PV power generation variability caused by different weather regimes will become substantially more critical, making the investigations of optimized spatial deployment of future PV systems highly relevant.

Therefore, this study aims to utilize climate information to suggest future PV capacity additions that reduce weather-induced generation variability. The study region is Europe and includes 36 countries covered by the European network of transmission system operators for electricity. We begin to assess the status quo in 2019 and subsequently analyze projections for 2030 and 2050 based on current National Energy and Climate Plans (NECPs) and an estimate for 2050 by the Energy Watch Group (Ram et al., 2017). In addition to computing the consequences of current plans, we highlight that coordinated approaches can substantially reduce multiday generation variability by introducing a numerical method that minimizes generation variability.

2. Data and Methods

Section 2.1 details the data entering the study, notably regarding meteorology, PV production, and energy consumption. Section 2.2 describes the methods successively applied to the data, from weather regime identification to formulating and solving the problem of optimal spatial deployment of PV capacities.

2.1. Data

2.1.1. ERA5

We define weather regimes based on 500 hPa geopotential height from the ERA5 reanalysis, published by the European Centre for Medium-Range Weather Forecasts (ECMWF; Hennermann & Yang, 2018; Hersbach et al., 2018). ERA5 provides hourly data with an appropriate spatial resolution (around 30 km grid size in Europe). To capture the large-scale circulation over Europe, we evaluate the larger Europe-North Atlantic region

(80°W–40°E, 30°–90°N). We use 41 years of data from January 1979 until June 2020 to account for inter-annual and decadal variability.

2.1.2. Renewables.ninja

Country-level PV capacity factors are taken from renewables.ninja. A detailed description of the underlying Global Solar Energy Estimator can be found in Pfenninger and Staffell (2016). We use European country-specific capacity factors provided by Renewables.ninja based on the reanalysis data set MERRA-2 covering 1985–2016. Note that ERA5-based capacity factors in renewable.ninja are currently not yet available. The unit-less capacity factor describes the ratio of actual generation relative to rated capacity. It is defined as:

$$\mathrm{CF} = P \,/\, \mathrm{IC} \tag{1}$$

For example, a capacity factor of one means that a PV system operates under perfect conditions and always produces its maximum output. In contrast, a capacity factor of zero indicates that no electricity is produced. For European countries, PV systems' average yearly capacity factors lie roughly between 0.1 and 0.2.

2.1.3. Installed PV Capacities

To compute actual national PV power generation from current capacity factors, we use installed capacities provided by IRENA (IRENA, 2020b). To assess future configurations, we use the NECPs in which countries define capacity targets until 2030. When NECPs are not available (see Section 6 Data Availability for country list), we consider individual national plans or, as a last resort, apply the average PV installed capacity growth rate until the year 2030 from all EU countries to the currently installed PV capacities.

Furthermore, we take the estimate "where we need to be by 2050" by the Energy Watch Group for total PV installed capacity in Europe 2050 (Ram et al., 2017).

2.1.4. Electricity Consumption Data

We use hourly electricity consumption data from Open Power System Data (Wiese et al., 2019) and fill gaps with data from the statistical office of the European Union (Eurostat, 2021). Since data availability differs per country, we take the latest fully reported year as the current total electricity consumption (range between 2016 and 2019).

2.2. Method

An overview of all steps used in the approach to reduce multiday PV power generation variability is given in Figure 1 below. A more detailed explanation of how the method finds a distribution of PV systems that reduces the variability is provided in the following subsections.

2.2.1. Weather Regime Classification

The weather regime classification consists of multiple steps. We begin with a daily resampling of the hourly geopotential height data and apply a 10-day Butterworth lowpass filter (Virtanen et al., 2020) (2nd order, critical frequency of 1/10d) to focus on variability over multiple days (Figure 1, steps 2 and 3). The filtered daily means (z_d) are used to calculate standardized anomalies (z_norm_d) as:

$$z\_\mathrm{norm}_d = (z_d - z_{d,\mathrm{mean}}) \,/\, z_{d,\mathrm{std}} \tag{2}$$

where $z_{d,\mathrm{mean}}$ ($z_{d,\mathrm{std}}$) denotes the climatology (standard deviation) over the 41 years of ERA5 data of the daily mean geopotential height, computed as a centered running mean over a window of 30 days. This approach removes the seasonal cycle amplitude by division with the standard deviation. Removing the amplitude caused by the seasonal cycle clears the way to define the WR year-round.

Our choice to use a 30-day running window for the reference climatology and standard deviation calculations differs from other studies. Often, investigations are made for weather regimes in winter where a correction for the seasonality is not needed. Others are using 90-day averaging periods (Grams et al., 2017). Still, since our interest focuses on multiday timescale, this is rather long and increases the probability that the impact of the seasonal cycle signal is relatively high.

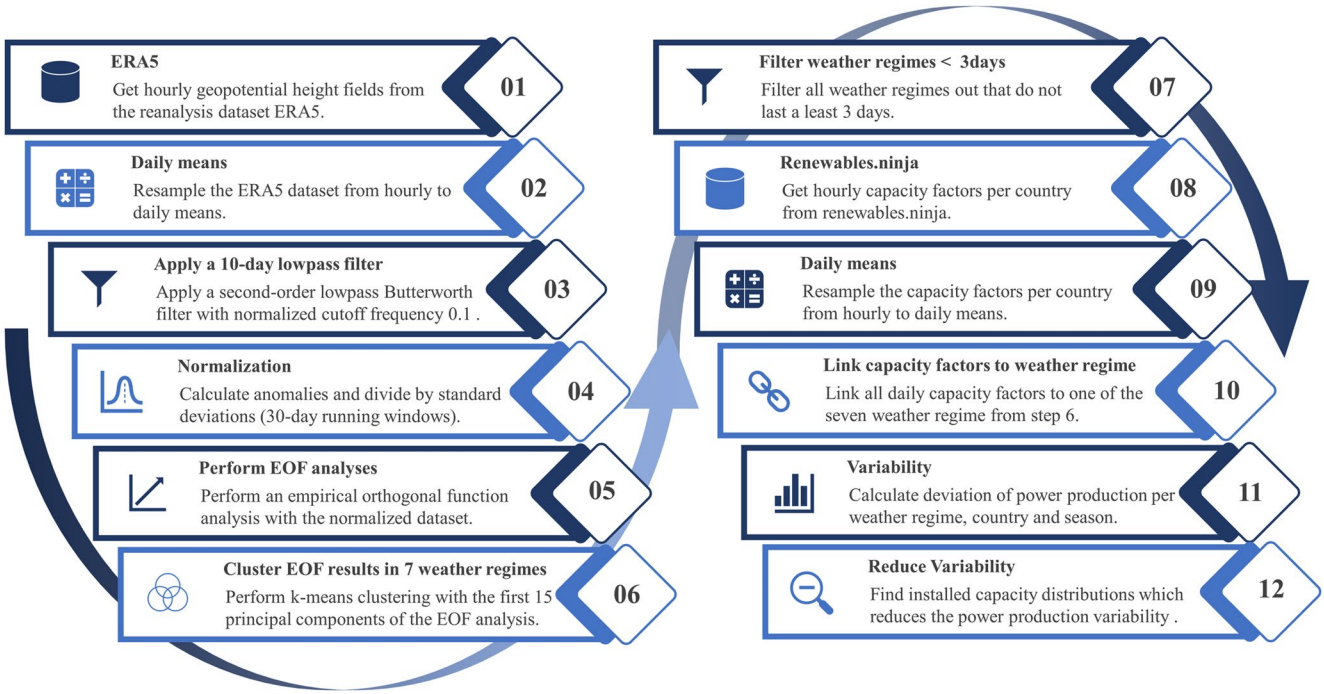

Figure 1. Overview of the approach to derive the weather regimes, link the country-specific capacity factors, and find a distribution that reduce the photovoltaic power generation variability.

For the weather regime classification (Figure 1, step 5 and 6), we use latitude weighted EOF analysis (Dawson, 2016) to identify the 16 leading patterns that explain around 90% of the variance and k-means clustering (Pedregosa et al., 2011) to map individual days to a prevailing EOF. In the Euro-Atlantic region, four clusters are commonly used to define weather regimes (Cassou, 2008; Michelangeli et al., 1995; van der Wiel et al., 2019), which yields in the weather regimes negative and positive phase of the North Atlantic Oscillation, the Scandinavia high and the Atlantic ridge. However, according to Grams et al. (2017), the optimal number of clusters to define weather regime year-round is seven, and we also choose seven clusters to enable direct comparison/combination. Furthermore, we exclude short-lasting weather regimes (less than 3 days) and assign these days to a separate weather regime hereafter refer to them as "no-regime" (Figure 1, step 7). This is done by checking the time-series after the clustering and finding all days where a weather regime does not prevail for at least three subsequent days and assigning them to "no-regime."

2.2.2. Capacity Factors and PV Power Generation Variability

The capacity factors data set is also resampled to daily means to derive multiday PV power generation variability (Figure 1, step 9). Since capacity factors follow a strong seasonal cycle, we analyze them separately for each season. The seasons are defined with the months December, January, February (DJF) for winter—March, April, May (MAM) for spring—June, July, August (JJA) for summer and September, October, November (SON) for autumn. We then link capacity factors to the different weather regimes (Figure 1, step 10) and calculate mean capacity factors per weather regime, country, and season ($CF_{wr,country,season}$). The difference between these mean capacity factors per weather regime and the mean capacity factors for the whole season of a country ($CF_{country,season}$) determines whether the weather regime exhibits over- or underproduction relative to the mean (Equation 3).

$$\Delta CF_{wr,country,season} = CF_{wr,country,season} - CF_{country,season} \tag{3}$$

Multiplication of capacity factors with installed capacities yields power output (Equation 1). This can be used to expand Equation 3, which gives the total deviation of PV power generation of Europe per weather regime and season (Figure 1, step 11).

$$\Delta P_{wr,Europe,season} = \sum_{country} \left(\Delta CF_{wr,country,season} \times IC_{country}\right) \tag{4}$$

where $IC_{country}$ is the installed PV capacity per country (W).

We use Equation 4 as a metric for the variability, which forms the basis for the following optimization. To understand Equation 4, we assume that it is zero for a specific weather regime and season. In that case, the respective weather regime and season's PV power generation equal the season's mean PV power generation. If the results for every weather regime and season of Equation 4 are zero, each season's PV power generation is, on average, constant across the different weather regimes. That would imply that the multiday variability induced by weather regime transitions is zero, reducing the challenge of considering the PV power generation variability for power grid balancing purposes.

Considering seven weather regimes plus no regime and four seasons implies 32 results of Equation 4 for the variability. To consolidate these 32 results, we introduce the mean and maximum PV power generation variability. The mean PV power generation variability is defined as the sum of the absolute changes in mean PV power generation resulting from the transition from one weather regime to another, weighted with the corresponding frequency of the transition as:

$$\text{mean\_var} = \sum_{i=0}^{n}\sum_{j=0}^{n}\left(\left|\left(P_{\text{wr}_i,\text{Europe,season}} - P_{\text{wr}_j,\text{Europe,season}}\right)\right| \times f_{i,j}\right) \tag{5}$$

where $n = 7$ is the total number of weather regimes, $P_{\text{wri,Europe,season}}$ is the mean PV power generation for a specific weather regime wr_i and season, $f_{i,j}$ is the frequency of the transition from weather regime i to j. The maximum PV generation variability is defined as the maximum difference of mean PV power generation between two weather regimes per season:

$$\text{max\_var} = P_{\text{wr}_{\max},\text{Europe,season}} - P_{\text{wr}_{\min},\text{Europe,season}} \tag{6}$$

Total mean and maximum PV power generation variability are defined as the average of the obtained results from Equation 5 and Equation 6 over the whole season.

2.2.3. Variability Reduction With Optimized Installed PV Capacity Distribution

To determine an installed capacity distribution that minimizes PV power generation variability, we use Equation 4 for every country, season, and weather regime in a linear least-square problem with an upper and lower bound on the variables (Virtanen et al., 2020) (Figure 1, step 12):

$$\text{minimize}\, 0.5 \times ||A\vec{x} - \vec{b}||^2 \quad \text{subject to}\, lb \le x \le ub \tag{7}$$

where A is the coefficient matrix, x is the solution, b is the target vector, lb is the lower bound of the solution x, and ub is the upper bound of the solution x.

The coefficient matrix A is defined with $\Delta CF_{\text{wr,country,season}}$ from Equation 3:

$$A = \begin{pmatrix} \Delta CF_{\text{WR1,AL, winter}} & \cdots & \Delta CF_{\text{WR1,SK,winter}} \\ \vdots & \ddots & \vdots \\ \Delta CF_{\text{WRX,AL,autumn}} & \cdots & \Delta CF_{\text{WRX,SK,autumn}} \end{pmatrix} \tag{8}$$

where, for instance, the first element of the matrix $\Delta CF_{\text{WR1,AL,winter}}$ is the capacity factor anomaly of weather regime 1, in Albania in winter. The columns of A are associated with the 36 countries considered, whereas the eight weather regimes and four seasons translate into the 32 rows of A.

The target vector $\vec{b}$ is set to zero, reducing the variability within one weather regime and season as much as possible and therefore also reducing the variability from one weather regime to another:

$$\vec{b} = [0, \ldots, 0] \tag{9}$$

The result of this method is the vector $\vec{x}$ which contains the installed capacity for each country:

$$\vec{x} = [IC_{AL}, \ldots, IC_{SK}] \tag{10}$$

Table 1
Overview of the Three Scenarios to Analyze Photovoltaic (PV) Power Generation Variability Reduction Potentials

Scenario	Description
Variability only	Reduce PV power generation variability while keeping total PV generation in 2030/2050 unchanged
Variability and Costs	Simultaneously reduce installed capacity (i.e., installation cost) and PV power generation variability while keeping total PV generation in 2030/2050 unchanged
Variability and Autarky	Reduce PV power generation variability while keeping total PV generation in 2030/2050 unchanged and ensuring 10%/30% of demand is met locally

The method to perform the minimization is the Trust Region Reflective algorithm (Branch et al., 1999). To avoid unrealistic decommissioning of existing PV panels, we set the lower bound to the current (2019) installed PV capacity per country (unless explicitly mentioned in the scenarios below). The upper bound is always set to the roof-top mounted PV potential per country (Tröndle et al., 2019).

2.2.4. Scenarios

Besides reducing PV power generation variability, we add constraints to the optimization, such as a minimum power generation on a European scale, a certain level of autarky per country or a limit on total capacity addition to control associated installation costs. To consider these trade-offs, we analyze three scenarios summarized in Table 1.

The scenario constraints are added row and element-wise to the coefficient matrix A (Equation 8) and the target vector $\vec{b}$ (Equation 9). They act as additional equations within our linear least-square problems.

To meet the requirements of the different scenarios and obtain better control over our linear least-square problem, we introduce a weighting vector $\vec{w}$:

$$\vec{w} = [w_0, \ldots, w_x] \tag{11}$$

where $\vec{w}$ is the weight assigned to the equations defined with the coefficient matrix A and the target vector $\vec{b}$. The weighting vector is useful to consolidate the various orders of magnitudes of our equations. For instance, the first 32 rows are of the same order of magnitude because they all describe the PV power generation variability. While an added constraint minimize total European PV generation would be larger. To apply the weighting vector, the square root of its elements is taken as elements of a diagonal matrix and is multiplied with the coefficient matrix A and the target vector $\vec{b}$, before solving the optimization problem:

$$A_w = A \times \begin{pmatrix} \sqrt{w_0} & \cdots & 0 \\ \vdots & \ddots & \vdots \\ 0 & \cdots & \sqrt{w_x} \end{pmatrix} \tag{12}$$

$$\vec{b}_w = \vec{b} \times \begin{pmatrix} \sqrt{w_0} & \cdots & 0 \\ \vdots & \ddots & \vdots \\ 0 & \cdots & \sqrt{w_x} \end{pmatrix} \tag{13}$$

In the following, we introduce the already mentioned scenarios for capacity allocation in the future in greater detail.

2.2.4.1. Scenario 1: Variability Only

The objective of the scenario "Variability only" is to minimize the multiday PV power generation variability while the total power generation with PV systems in Europe must remain the same as estimated with the NECPs for 2030 or with the estimate for 2050 by the Energy Watch Group. We compare variability based on current plans and based on an optimized distribution of installed PV capacities that produces the same amount of electricity,

showing the total potential of the PV generation variability reduction with an optimized installed capacity distribution without additional constraints.

To implement this scenario, we add all the mean capacity factors per country as an additional row to the coefficient matrix A and the total PV power generation as an additional element to the target $\vec{b}$.

$$A_{\text{var}} = \begin{pmatrix} \dots & \dots & \dots \\ \vdots & \ddots & \vdots \\ \text{CF}_{\text{AL}} & \dots & \text{CF}_{\text{SK}} \end{pmatrix} \tag{14}$$

where A_{var} is the coefficient matrix for the scenario "Variability only" (expansion of Equation 8) and CF_{AL} and CF_{SK} are the mean capacity factors for Albania and Slovakia, which are alphabetically the first and last considered countries.

$$\overrightarrow{b\_\text{var}} = [\dots, \text{tot}_{\text{prod}}] \tag{15}$$

where b_var is the target vector for the scenario variability (expansion of Equation 9), and tot_{prod} is the total PV power generation estimated for 2030 or 2050, respectively.

The weighting vector is chosen such that the equation considering the total PV power generation gets ten times as much weight as each equation considering variability.

2.2.4.2. Scenario 2: Variability and Costs

In addition to reducing generation variability, this scenario also minimizes installed PV capacity and, therefore, associated costs while producing the same amount of electricity as estimated with the installed PV capacity planned in the NECPs for 2030 or with the upscaled estimates for 2050. The constraint for the PV power generation is added similarly as before. We include the minimization installed PV capacities by adding a row with ones to the coefficient matrix A and zero as an element to the target vector $\vec{b}$. This equation penalizes capacity additions and thus acts as an incentive to generate energy with minimal installed capacity. The weighting vector for the scenario costs is chosen, such as the equation considering the total installed capacity gets about ten times less weight than the equation considering variability and the equation considering total PV power generation.

2.2.4.3. Scenario 3: Variability and Autarky

This scenario seeks to minimize PV generation variability, while each country must generate 10% of its electricity consumption with PV systems itself in the year 2030 or 30% in the year 2050. We use historical consumption data (Section 2.1.4) because we focus on variability reduction potentials if we enforce a less clustered distribution of installed capacities rather than on actual percentual coverages per country's consumption. The scenario "Variability and Autarky" is constructed like the scenario "Variability only," but instead of the currently installed PV capacities for each country as lower bound, scenario "Variability and Autarky" uses 10% of the yearly consumption per country (30% for 2050) divided by the capacity factors per country as lower bound.

$$lb_{\text{country}} = 10\% \times \text{load}_{\text{country}} \,/\, \left(\text{CF}_{\text{country}} \times 365\text{d} \times 24\frac{h}{d}\right) \tag{16}$$

where $\text{lb}_{\text{country}}$ is the lower bound for the installed PV capacity per country (W), $\text{load}_{\text{country}}$ is the yearly electricity consumption per country (Wh), and $\text{CF}_{\text{country}}$ is the capacity factor per country (unitless).

3. Results and Discussions

3.1. Weather Regimes and Associated Capacity Factors Anomalies

Figure 2 presents the weather regimes, their likelihood of occurrence and their relation to the country-specific capacity factors per season. We find that weather regimes have strong control over country-specific capacity factors. While positive geopotential height anomalies (anticyclones) cause positive capacity factor anomalies, negative geopotential height anomalies (cyclones) cause negative capacity factor anomalies. These relations match expectations because anticyclones are related to descending air, clear sky conditions, and therefore

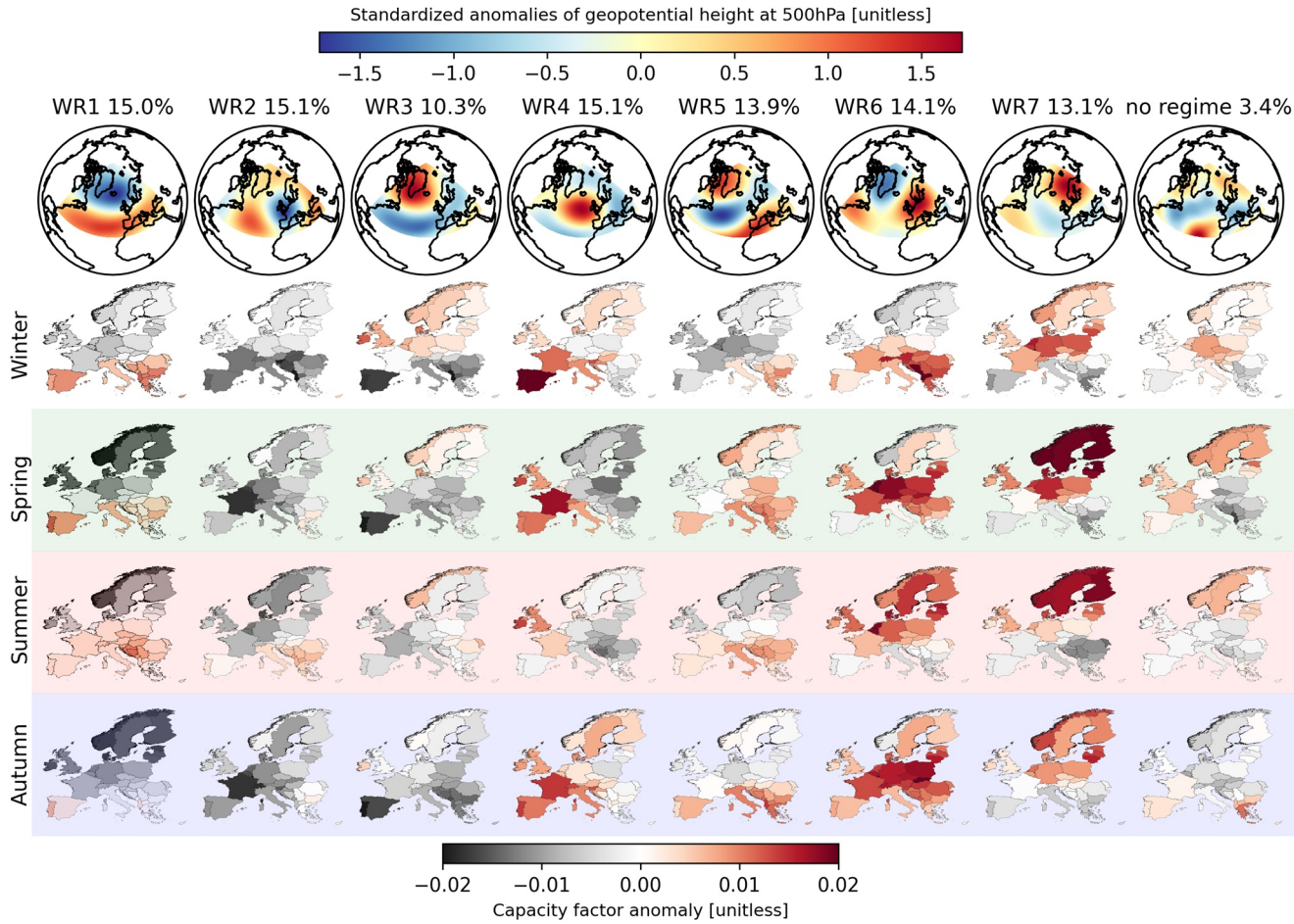

Figure 2. Link between the derived seven weather regimes and the photovoltaic capacity factor anomalies per country and season. The first row shows standardized anomaly fields of geopotential height at 500 hPa for each weather regime and their frequency of occurrence. The linked capacity factor anomalies per country are shown separately for each season. They are calculated as the difference to the corresponding seasonal mean: winter (December, January, February), spring (March, April, May), summer (June, July, August), and autumn (September, October, November).

enhanced capacity factors. In contrast, cyclones usually induce enhanced cloud cover and reduced surface solar radiation, thereby decreasing capacity factors. The relation between the derived weather regimes and the most important variables to determine the capacity factors, namely surface solar radiation, and 2-m temperature, can be found in Figure S1 in Supporting Information S1.

An essential outcome of the results presented in Figure 2 is that cyclonic/anticyclonic conditions often affect only a part of Europe. Therefore, positive and negative capacity factor anomalies usually co-exist in different parts of Europe within one weather regime, suggesting that weather-induced below-average PV production in one region can be buffered by a corresponding above-average production from another region if capacities are distributed, taking this information into account. There are, however, a few cases where negative capacity factor anomalies prevail all over Europe (e.g., WR2 in winter). In such cases, it is impossible to mitigate multiday PV power generation variability by an optimized distribution.

3.2. Variability — Current Situation (2019)

The European installed PV capacity in 2019 amounts to 131.2 GW (IRENA, 2020b). Most of the capacity is installed in Western Europe, with Germany as the leading country. Annual mean PV power generation in 2019 equals 17.5 GW (153 TWh/y) with substantial seasonality: 8.6 GW in winter, 21.7 GW in spring, 25.7 GW in summer, and 14.0 GW in autumn. Transitions between weather regimes result in multiday PV generation variability. For 2019, we quantify the associated mean variability at 0.9 GW, calculated as the average change of PV

power generation upon a weather regime transition. This number roughly corresponds to the rated capacity of one nuclear power plant and equals 5.1% of mean PV production. The maximum variability, defined as the maximum difference between weather regimes, amounts to 3.0 GW, corresponding to 17.1% of mean PV power generation. These variabilities are non-negligible within the context of PV power generation. Yet, they are small compared to the current total power production in Europe (Jäger-Waldau, 2019). But this will change with the growing system-wide importance of PV generation. According to the plans by NECPs, installed PV capacity triples by 2030 and continues to increase sharply thereafter. The projection to 2050 (Ram et al., 2017), which informs our future scenarios, suggests a 19 fold increase from 2015 until 2050. Other scenarios even assume stronger capacity growth (SolarPower Europe and LUT University, 2020). The growing relevance of PV for total power generation implies growing relevance of associated production variability.

3.3. Variability 2030 and Its Reduction Opportunities

The NECP capacity additions by 2030 leave the current pattern of installed capacities unchanged: most capacity is still located in Western Europe (Figure 3a). Consequently, we find that along with the tripling of total capacity, the mean and maximum variability scale in concert and also roughly triple, to 2.7 and 8.5 GW. When compared to a more distributed allocation of capacity, such a distribution constitutes a cluster risk because weather regimes often affect central and western Europe equally (see Figure 2).

We thus seek to explore the potential for variability reduction via informed siting of additional PV capacity. To do so, we demand the same PV power generation of 52.3 GW as in NCEP 2030 (scenario "Variability only") and perform a linear optimization of added capacity. In contrast to NECPs, this method favors additional capacities in southeastern and northwestern Europe (see Figure 3b), thereby almost halving the mean variability from 2.7 to 1.5 GW. Similarly, the maximum variability reduces from 8.5 to 5.2 GW (see also Figure 4 for a seasonal overview). These variability reductions are achieved with less installed PV capacity (373.6 vs. 386.5 GW), reflecting that the optimization identifies superior locations in terms of both total generation and low variability. It should be noted that the actual distribution of installed capacities is currently not decided on a European level but on a national level. Implementing planning and policies along the lines suggested in this paper thus also represents an implementation challenge in addition to a meteorological challenge. We provide a more detailed overview of all results for the year 2030 in Table A1 in Appendix A.

If cost minimization is explicitly added to the optimization, we observe a shift from the southeastern/northwestern distribution to a southeastern/southwestern distribution (Figure 3c). This configuration requires 33.7 GW less installed capacity than the "Variability only" scenario to produce the same amount of electricity. Reductions in mean variability (from 2.7 to 1.8 GW) and maximum variability (from 8.5 to 6.1 GW) are still pronounced, yet somewhat weaker compared to the pure variability minimization, in line with expectations (see also Figure 4). We find that the scenario "Variability and Costs" decreases mean variability by 27% compared to 39% in the "Variability only" scenario. These findings highlight synergies between reducing PV power generation variability and lowering investment costs. Nevertheless, a thorough analysis reveals limitations: capacity is almost exclusively added in three countries (Cyprus, Greece, and Spain). Seasonal examination (Figure 4) indicates that variability is only slightly reduced in winter when electricity demand is highest.

The two scenarios examined so far mainly added capacity in geographically distant regions of Europe, like Greece or Scandinavia. With such a geographically distant distribution, one needs to mention the assumptions of an unlimited power grid again. Further analysis regarding the power grid is necessary to set the results into context. In practice, such a distribution of power production would require substantial grid reinforcement on the continental scale and require collective willingness to act from many countries. This motivates another scenario that includes countries willingness to maintain certain levels of self-sufficiency. In the scenario "Variability and Autarky," we therefore demand that 10% of the yearly country-specific consumption must be produced with local PV systems in 2030. The resulting flatter distribution of this scenario is shown in Figure 3d. All countries get installed capacities needed to cover at least 10% of their yearly consumption. Additional capacities required to meet the total annual mean production target of 52.3 GW are again distributed to southeastern and northwestern Europe. The flatter distribution has only a minor impact on the variability reduction potential. It drops by about 10% compared to the "Variability only" scenario and yields mean and maximum variability of 1.9 and 6.1 GW, respectively. The findings of scenario "Variability and Autarky" indicate the potential for large PV power plants in key countries to reduce variability. Furthermore, it shows that reduced PV power generation variability can be

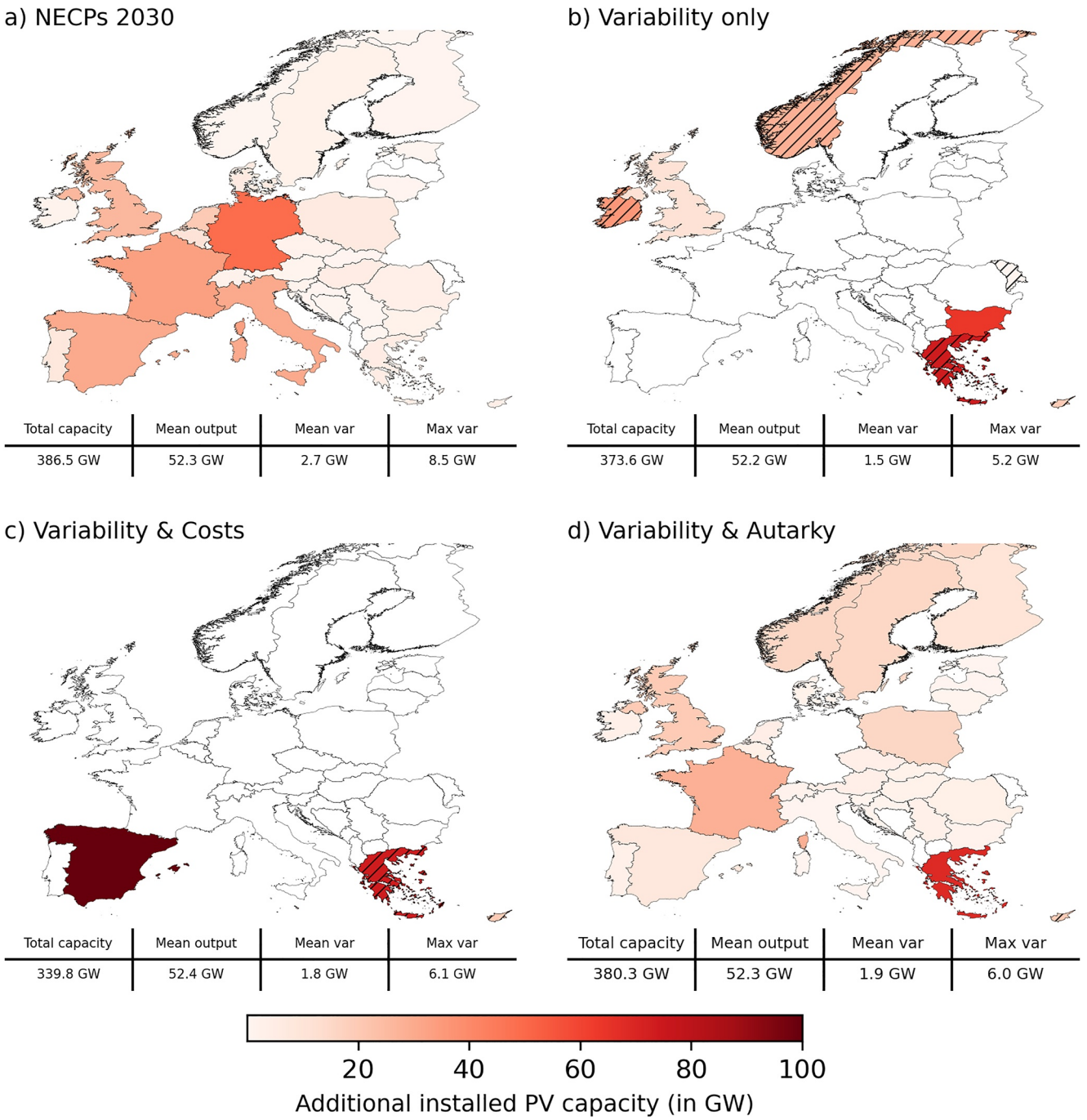

Figure 3. Additional installed photovoltaic (PV) capacity distributions planned for 2030 (National Energy and Climate Plans, NECPs) and resulting from the three scenarios "Variability only," "Variability and Costs," and "Variability and Autarky." Hatched countries indicate that the upper bound (potential for roof-top mounted PV systems) is reached.

achieved jointly with some degree of self-sufficiency, thus it may need less continental transmission infrastructure, with about the same total installed capacity as envisaged in NECPs 2030 plans. The corresponding absolute installed PV capacity distributions to the here presented additional installed capacities in Figure 3 can be found in Figure S2 in Supporting Information S1.

A seasonal perspective (Figure 4) shows that PV generation variability in absolute terms tends to be highest in mid-season (spring and autumn) for NECPs and all scenarios. All scenarios reduce the variability in each season,

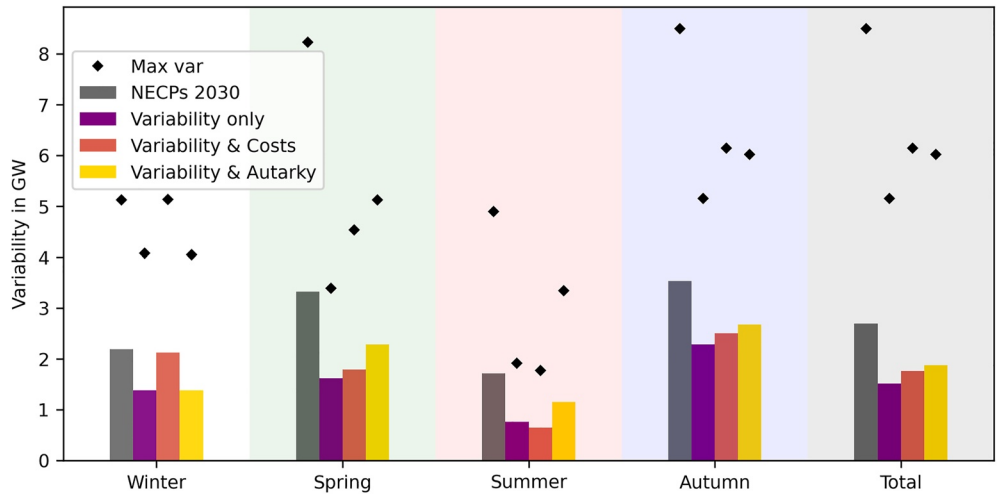

Figure 4. Mean (bars) and maximum (black markers) consolidated (over all weather regimes) variability per season and overall (total). In gray, the estimated variability with the planned installed capacities for 2030 (National Energy and Climate Plans, NECPs) and in color the estimated variability with the installed capacity distribution for scenario "Variability only," "Variability and Costs," and "Variability and Autarky," respectively.

demonstrating that many different improvements to current plans exist that combine different additional goals. As expected, the largest reductions can generally be achieved with the "Variability only" scenario. Summer is an exception, where the scenario "Variability and Costs" causes stronger variability reductions by concentrating installed capacities to Southern Europe, where weather in summer is more constant. The variability of this scenario in winter is, by contrast, nearly identical to the variability estimated with the NECPs. The findings highlight the need for seasonal analysis, especially if the investigation were expanded to include electricity demand and other power generating technologies with potentially different overall seasonality than PV power generation. A detailed overview of the deviation of PV power generation from the seasonal mean per weather regime and season in 2030 can be found in Figure S3 in Supporting Information S1.

3.4. Variability 2050 and Its Reduction Opportunities

The estimated installed PV capacity of 1.94 TW for 2050 (Ram et al., 2017) results in total mean and maximum variabilities of 13.9 and 43.8 GW if capacity is added using the same relative distribution per country as in 2019. Similar to 2030, variability minimization with equal production (scenario "Variability only") still places most installed capacities to southeastern/northwestern Europe. However, since total installed capacities are much higher in 2050 than in 2030, the maximum country capacities are more often reached (hatched countries in Figure 5). The method reacts by placing additional capacity first in neighboring countries and second to northeastern and southwestern Europe, following the general pattern that capacity factor anomalies in these two regions are often anticorrelated (Figure 2). The reduction potentials (in per cent) of scenario "Variability only" is slightly lower in 2050 than in 2030, which is related to the mentioned fact that ideal locations are already full exploited, requiring sub-optimal additions. Nevertheless, the mean (maximum) variability is decreased by 4.7 GW (13.2 GW). We provide a more detailed overview of all results for the year 2050 in Table A2 in Appendix A.

In the joint "Variability and Costs" optimization, the mean variability is reduced by 2.2 GW, and the maximum variability is reduced by 9.6 GW (Figure 5c). Additional capacity is generally installed into Southern countries where capacity factors are higher. Consequently, 197.3 GW less capacity is required to produce the same amount of electricity compared to the scenario "Variability only." Compared to 2030, these results indicate that joint variability and cost reduction becomes more challenging with increased installed PV capacity. For instance, the optimization still reduces variability but to a smaller degree (roughly half of the mean reduction potential and two thirds of the maximum reduction potential of scenario "Variability only"). The benefit in reducing the costs compared to 2030 has also decreased. While the same amount of electricity could be produced with 18% less additional installed PV capacity in 2030, this reduction drops to 13% in 2050. The cause for this deterioration is

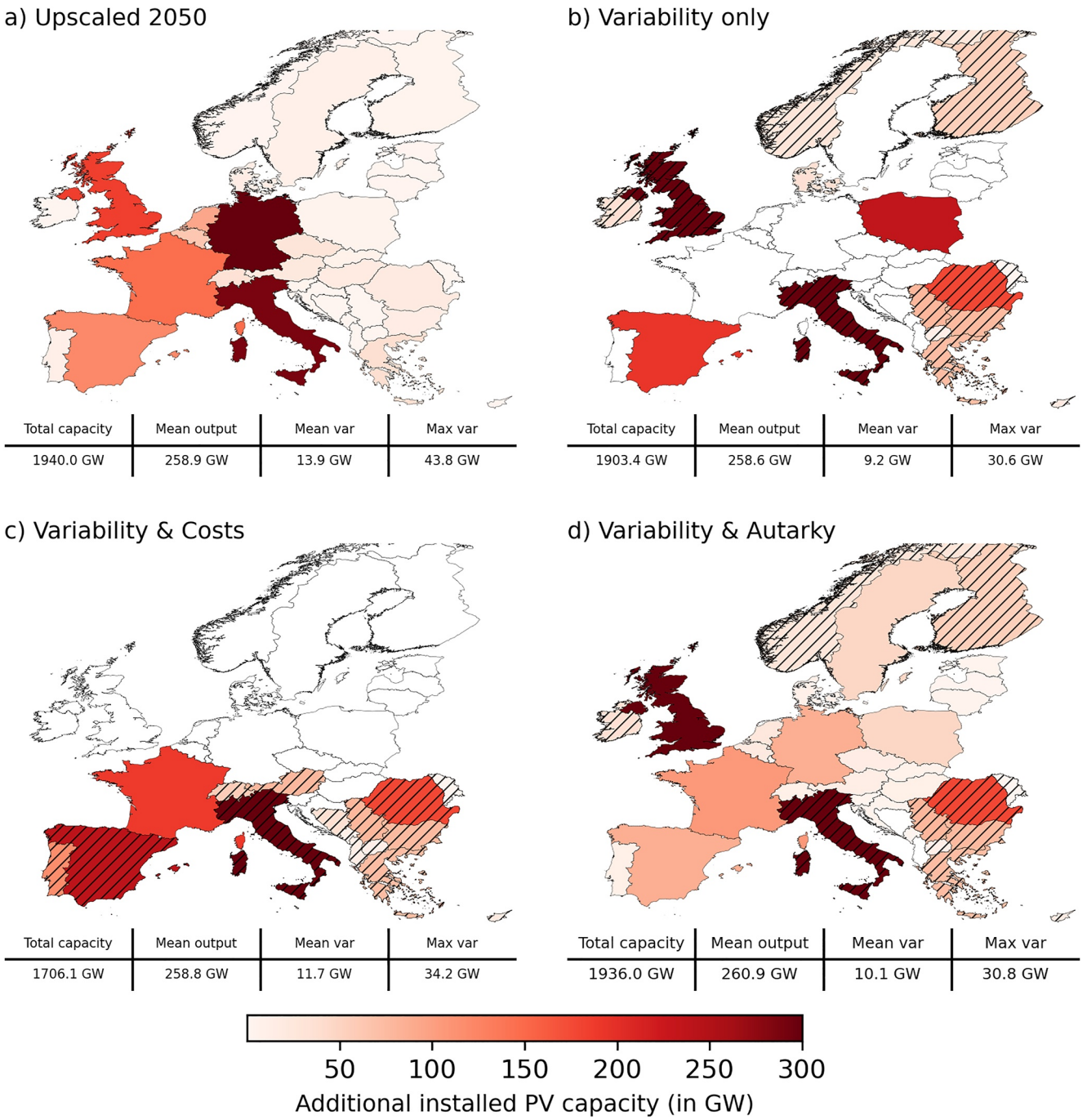

Figure 5. Additional installed photovoltaic (PV) capacity distributions upscaled for 2050 and resulting from the three scenarios "Variability only," "Variability and Costs," and "Variability and Autarky." Hatched countries indicate that the upper bound (potential for roof-top mounted PV systems) is reached.

again that upper bounds per country are more often hit, leading to more capacity in northern countries with lower capacity factors.

Lastly, the scenario "Variability and Autarky" that assumes 30% autarky levels in 2050 yields a flatter distribution (Figure 5d). This spatial diversification causes a mean (maximum) variability reduction of 3.8 GW (13.0 GW), which is comparable to the scenario "Variability only." This result demonstrates the balancing potential of a flatter distribution where the countries are self-sufficient to a certain degree while also decreasing the need for power line expansion, but it is still possible to substantially reduce the variability. When planning larger solar

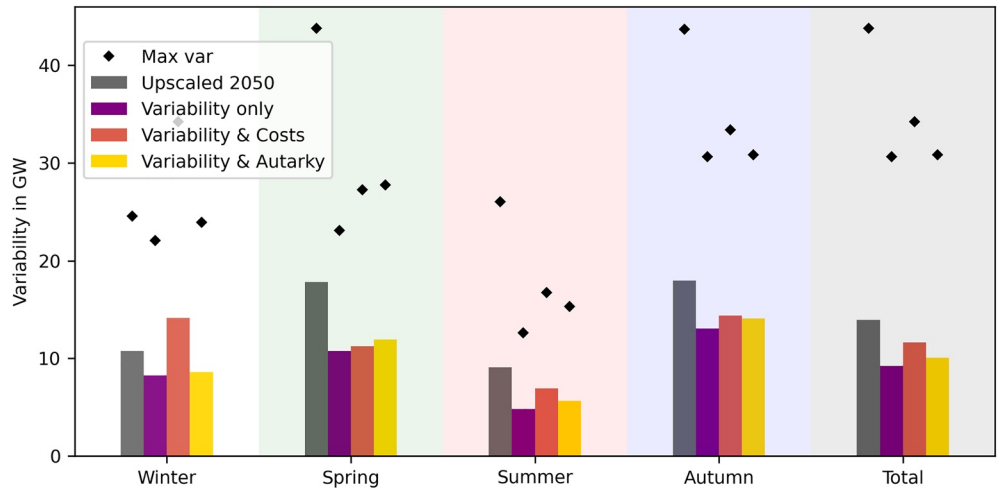

Figure 6. Mean (bars) and maximum (black markers) consolidated (over all weather regimes) variability per season and overall (total). In gray, the estimated variability with the upscaled installed capacities to the year 2050 and in color the estimated variability in 2050 with the installed capacity distribution for scenario "Variability only," "Variability and Costs," and "Variability and Autarky," respectively.

power systems and their location, these results may also be of interest. Even in an already present flat installed PV capacity distribution, a new large solar power system in a key country like Greece could reduce the PV power production variability. The corresponding absolute installed PV capacity distributions to the here presented additional installed capacities in Figure 5 can be found in Figure S4 in Supporting Information S1.

A closer look at the variabilities per season (Figure 6) shows that all scenarios reduce the variabilities in every season except scenario "Variability and Costs" in winter, where the variability even increases. The results are similar to the results for 2030, where the variability in winter could not be reduced substantially. A possible explanation is the equivalent effect of weather regimes to capacity factors for southern countries in winter. It is reasonable to place most installed capacities to the South for cost consideration. And it is also for variability reduction considerations in most seasons, but not for winter, where, unfortunately, electricity demand is still highest. However, the relative variability of the other two scenarios and the upscaled variability show similar results as for 2030. Scenario "Variability only" reduces the variability the most in every season and total. Interestingly scenario "Variability and Autarky" now reduces the variability more than scenario "Variability and Costs" and is almost in reach with scenario "Variability only." A detailed overview of the deviation of PV power generation from the seasonal mean per weather regime and season in 2050 can be found in Figure S5 in Supporting Information S1.

3.5. Comparison and Combination With Wind Power Production Variability

Given current strategies for 2030, energy system operators will need to consider power generation fluctuations of 8.5 GW from solar PV, which will correspond to 16% of the wind power variability (Grams et al., 2017). In 2050 these numbers could significantly increase to 43.8 GW (maximum variability), comparable to the 89.6 GW wind power production variability that follows from upscaling the Grams et al. (2017) estimates using wind capacities by the Energy Watch Group (Ram et al., 2017). In such future systems, PV generation variability matters. For instance, the 13.2 GW PV variability reduction that we achieved with an optimized distribution would no longer be negligible and could substantially help to balance the power grid on a multiday timescale.

Moreover, positive effects from combining different renewables could be strategically used in optimized approaches to ensure that demand always equals electricity production. Others analyzed the energy system's stress caused by wind and PV production and their dependency on weather (Bloomfield et al., 2020; van der Wiel et al., 2019) and reported that blocking situations have lower than average power production with wind and PV and higher than average energy demand. Our results suggest that PV power production is higher on average

during blocking situations. For instance, PV power generation is high during European blocking (WR5). In contrast, wind power production is low in this regime (Grams et al., 2017), highlighting the potential to reduce the energy system's stress via mixed technology portfolios, including PV and wind power.

4. Conclusions and Outlook

PV power generation is subject to significant fluctuations because of its weather dependency. Currently, multiday fluctuations are of minor importance to the power grid because PV power generation in Europe is small compared to the power produced by other technologies. But with the continued growth of installed PV capacity, dealing with the weather-dependent variability at these longer timescales will become increasingly essential. We report that in 2030, the change in mean PV power generation from one weather regime to another could amount to up to 8.5 GW. Consequently, other power plants or storage facilities must generate this electricity to balance the power grid. We have shown that under the condition of an unlimited power grid (transmission), a southeastern/northwestern distribution of PV systems in Europe reduces this variability by roughly 40% to 5.2 GW. Furthermore, the investigations indicate that PV production variability and costs can be reduced simultaneously. It is feasible to reduce the variability projected for 2030 by roughly 30% with 10% less installed PV capacity. Requiring that each country produces 10% of its electricity consumption within its borders by PV turns out to be of little consequence concerning overall production and production fluctuations. This aspect is of interest as local power production and consumption may imply less cross-border transmission infrastructure.

Different studies propose that the installed PV capacity must increase massively toward 2050 to achieve a 100% renewable electricity-producing Europe (IRENA, 2020a; Ram et al., 2017; SolarPower Europe and LUT University, 2020). Based on one of these studies (Ram et al., 2017), we have estimated the maximum regime-to-regime variability in 2050 to be 43.8 GW. In the scenario foreseeing large PV capacity additions, the potential of roof-top mounted PV systems per country is repeatedly reached, and our method places additional installed PV capacities in countries where the variability reduction potential is smaller. Not being able to exploit the optimal locations lowers the potential to reduce the variability from 40% (2030) to 30% (2050). Nevertheless, these 30% yields a substantial reduction of 13.2 GW in absolute numbers, implying a significant need for backup infrastructure. With the estimates for 2050, it is still feasible to reduce variability and costs simultaneously. With 10% less installed PV capacity, we reduced the variability by roughly 15%. However, a closer look at seasons also showed the limit of the resulting southern distribution for this scenario. It reduces the variability in all seasons except winter, where it even increased, but electricity demand is highest. Finally, the examined scenario where 30% of the electricity demand must be covered with in-land PV production in 2050 reduced the variability by roughly 30%—indicating that a flatter distribution with less needed transmission is similarly effective as pure variability minimization.

To our knowledge, the present study is the first to examine the reduction of multiday PV power generation variability with a distribution of PV systems based on weather regime classification. Our method is extendable to cover additional (renewable) energy sources or constraints. For example, it may be used to address the combined variability reduction of PV and wind power. Another improvement of the presented method could be to use capacity factors on a smaller scale than country-specific ones. An analysis on a smaller scale would consider capacity factor differences within one large country and increase the number of locations where PV systems can be distributed. Furthermore, the applied weightings could be analyzed in more depth. For instance, a continuum of weights could be inserted, gradually shifting the weight from variability to the other constraints (cost, autarky) to develop a systematic overview of their impact.

We have shown that as the installed PV capacity increases in the future, the associated multiday variability in power production becomes substantial in absolute terms. Our results suggest that instead of further massive unplanned PV deployment, large benefits exist when using the variability reduction potential originating from a weather regime informed optimized distribution of PV systems. This meteorological understanding in power system planning will help achieve a carbon-neutral European energy system at feasible costs without undermining the security of supply. Optimal siting can be one component of a portfolio of measures to help balance renewable grids across the European continent—alongside storage, transmission, and demand-side flexibility. If we do not take this opportunity, the variable power input will be unnecessarily more extensive, and more research and innovation are needed to balance the power grid sustainably.

Appendix A

A more detailed overview of the scenarios' results can be found in Table A1 and A2. They have been separated into all results for 2030 (Table A1) and all results for 2050 (Table A2) to facilitate comparisons between the different scenarios for the same year.

Table A1
Detailed Overview of the Results With the National Energy and Climate Plans (NECPs) and the Three Scenarios for 2030

	NECPs 2030	Variability only	Variability and Costs	Variability and Autarky
Installed PV capacity (GW)	386.5	373.6	339.8	380.3
Mean PV production (GW)	52.3	52.2	52.4	52.3
Mean variability (GW)	2.7	1.5	1.8	1.9
Maximum variability (GW)	8.5	5.2	6.1	6.0
Mean variability/mean PV production (%)	5.2%	2.9%	3.4%	3.6%
Maximum variability/mean PV production (%)	16.3%	10.0%	11.6%	11.5%
Mean variability reduction (GW)	–	1.2	0.9	0.8
Maximum variability reduction (GW)	–	3.3	2.4	2.5
Mean variability reduction (%)	–	44.4	33.3	29.6
Maximum variability reduction (%)	–	38.8	28.2	29.4

Table A2
Detailed Overview of the Results Upscaled for 2050 and the Three Scenarios for 2050

	Upscaled 2050	Scenario variability	Scenario costs	Scenario autarky
Installed PV capacity (GW)	1,940.0	1,903.4	1,706.1	1,936.0
Mean PV production (GW)	258.9	258.6	258.8	260.9
Mean variability (GW)	13.9	9.2	11.7	10.1
Maximum variability (GW)	43.8	30.6	34.2	30.8
Mean variability/mean PV production (%)	5.4	3.6	4.5	3.9
Maximum variability/mean PV production (%)	16.9	11.8	13.2	11.8
Mean variability reduction (GW)		4.7	2.2	3.8
Maximum variability reduction (GW)		13.2	9.6	13.0
Mean variability reduction (%)		33.8	15.8	27.3
Maximum variability reduction (%)		30.1	21.9	29.7

Data Availability Statement

- All scripts and figures produced in this study can be found in the GitHub repository https://github.com/dmuehlemann/RPGV or via https://doi.org/10.5281/zenodo.5834042 with MIT license. The repository also contains the information on where the used research data can be downloaded to reproduce the work (similar to Section 2.1 data and below).
- The ERA5 hourly data on pressure levels used for the weather regime classification in the study are available at the Climate Data Store via https://doi.org/10.24381/cds.bd0915c6 (Hersbach et al., 2018).
- The country-specific capacity factors data set v1.1 used for calculating photovoltaic (PV) power generation in the study are available at https://www.renewables.ninja/downloads via https://doi.org/10.1016/j.energy.2016.08.060 with Creative Commons Attribution-NonCommercial 4.0 International (CC BY-NC 4.0) license (Pfenninger & Staffell, 2016).

- The installed capacities per country data used to compute actual national PV power generation in the study are available at IRENA Renewable Capacity Statistics 2020 via ISBN 978-92-9260-239-0 (IRENA, 2020b).
- The National Energy and Climate Plans used to assess future configurations in the study are available at European Commission website with Creative Commons Attribution 4.0 International (CC BY 4.0) license (European Commission, 2021).
- The hourly electricity consumption data set used for scenario autarky in the study are available at Open Power System Data via https://doi.org/10.25832/time_series/2020-10-06 with MIT License (Wiese et al., 2019).
- The second hourly electricity consumption data set used for scenario autarky in the study are available in Eurostat Data Browser with the online data code NRG_CB_E with Creative Commons Attribution 4.0 International (CC BY 4.0) license (Eurostat, 2021).
- The roof-top mounted PV potential per country data used as upper bound in the linear least-square problems in the study are available at Zenodo via https://doi.org/10.5281/zenodo.3246303 with Creative Commons Attribution 4.0 International (CC BY 4.0) (Tröndle et al., 2019).
- 3.3.1 of Matplotlib used for creating figures is preserved at https://doi.org/10.5281/zenodo.3984190, available via PSF license and developed openly at https://matplotlib.org/ (Hunter, 2007).
- v0.6.1 of geopandas used for creating maps with country based information is preserved at https://doi.org/10.5281/zenodo.3483425, available via BSD 3-Clause license and developed openly at https://geopandas.org/ (Jordahl et al., 2019).
- v0.17.0 of SciTools/cartopy used for creating weather regime maps is preserved at https://doi.org/10.5281/zenodo.1490296 available via LGPL-3.0 license and developed openly at https://scitools.org.uk/cartopy (Met Office, 2018).
- 1.4.0 of the eofs used for the empirical orthogonal function analysis is preserved at https://doi.org/10.5281/zenodo.2661604, available via GNU GPLv3 license and developed openly at https://ajdawson.github.io/eofs/v1.4/ (Dawson, 2016).
- 0.23.2 of the scikit-learn used for k-means clustering is preserved at https://scikit-learn.org/0.23/, available via BSD-3-Clause license and developed openly at https://scikit-learn.org/ (Pedregosa et al., 2011).

Acknowledgments
This work has received funding from the SENTINEL Project of the European Union's Horizon 2020 research and innovation program under grant agreement No. 83708. During large parts of this work, J. Wohland was funded through an ETH Postdoctoral Fellowship and acknowledged support from the ETH and Uniscientia foundations. The authors would like to thank Hannah Bloomfield for exchanging weather types in renewable energy applications.

References

Bloomfield, H. C., Brayshaw, D. J., & Charlton-Perez, A. J. (2020). Characterizing the winter meteorological drivers of the European electricity system using targeted circulation types. *Meteorological Applications*, *27*(1), 1–18. https://doi.org/10.1002/met.1858

Branch, M. A., Coleman, T. F., & Li, Y. (1999). Subspace, interior, and conjugate gradient method for large-scale bound-constrained minimization problems. *SIAM Journal on Scientific Computing*, *21*(1), 1–23. https://doi.org/10.1137/S1064827595289108

Brayshaw, D. J., Troccoli, A., Fordham, R., & Methven, J. (2011). The impact of large scale atmospheric circulation patterns on wind power generation and its potential predictability: A case study over the UK. *Renewable Energy*, *36*(8), 2087–2096. https://doi.org/10.1016/j.renene.2011.01.025

Cassou, C. (2008). Intraseasonal interaction between the Madden-Julian Oscillation and the North Atlantic Oscillation. *Nature*, *455*(7212), 523–527. https://doi.org/10.1038/nature07286

Dawson, A. (2016). eofs: A library for EOF Analysis of meteorological, oceanographic, and climate data. *Journal of Open Research Software*, *4*(1), 4–7. https://doi.org/10.5334/jors.122

Drücke, J., Borsche, M., James, P., Kaspar, F., Pfeifroth, U., Ahrens, B., & Trentmann, J. (2020). Climatological analysis of solar and wind energy in Germany using the Grosswetterlagen classification. *Renewable Energy*, *164*, 1254–1266. https://doi.org/10.1016/j.renene.2020.10.102

Ely, C. R., Brayshaw, D. J., Methven, J., Cox, J., & Pearce, O. (2013). Implications of the North Atlantic Oscillation for a UK-Norway renewable power system. *Energy Policy*, *62*, 1420–1427. https://doi.org/10.1016/j.enpol.2013.06.037

European Commission. (2019). The European green deal. Retrieved from https://ec.europa.eu/info/sites/default/files/european-green-deal-communication_en.pdf

European Commission. (2021). National Energy and Climate Plans. Retrieved from https://ec.europa.eu/info/energy-climate-change-environment/implementation-eu-countries/energy-and-climate-governance-and-reporting/national-energy-and-climate-plans_en

Eurostat. (2021). Supply, transformation and consumption of electricity. Retrieved from https://ec.europa.eu/eurostat/databrowser/view/nrg_cb_e/default/table?lang=en

Graabak, I., & Korpås, M. (2016). Variability characteristics of European wind and solar power resources—A review. *Energies*, *9*(6), 1–31. https://doi.org/10.3390/en9060449

Grams, C. M., Beerli, R., Pfenninger, S., Staffell, I., & Wernli, H. (2017). Balancing Europe's wind-power output through spatial deployment informed by weather regimes. *Nature Climate Change*, *7*(8), 557–562. https://doi.org/10.1038/nclimate3338

Hennermann, K., & Yang, X. (2018). *ERA5 data documentation*. European Centre for Medium-Range Weather Forecasts. Retrieved from https://confluence.ecmwf.int/display/CKB/ERA5%3A+data+documentation

Hersbach, H., Bell, B., Berrisford, P., Biavati, G., Horányi, A., Muñoz Sabater, J., et al. (2018). *ERA5 hourly data on pressure levels from 1979 to present*. Copernicus Climate Change Service (C3S) Climate Data Store (CDS). https://doi.org/10.24381/cds.bd0915c6

Huld, T., Gottschalg, R., Beyer, H. G., & Topič, M. (2010). Mapping the performance of PV modules, effects of module type and data averaging. *Solar Energy*, *84*(2), 324–338. https://doi.org/10.1016/j.solener.2009.12.002

Hunter, J. D. (2007). Matplotlib: A 2D graphics environment. *Computing in Science & Engineering*, *9*(3), 90–95. https://doi.org/10.1109/MCSE.2007.55

IRENA. (2020a). *Global renewables outlook: Energy transformation 2050*. International Renewable Energy Agency (IRENA).

IRENA. (2020b). *Renewable capacity statistics 2020*. International Renewable Energy Agency (IRENA).

Jäger-Waldau, A. (2019). *PV status report 2019, EUR 29938*. Publications Office of the European Union. https://doi.org/10.2760/326629

Jakubcionis, M., & Carlsson, J. (2017). Estimation of European Union residential sector space cooling potential. *Energy Policy*, *101*(May 2016), 225–235. https://doi.org/10.1016/j.enpol.2016.11.047

Jerez, S., Trigo, R. M., Vicente-Serrano, S. M., Pozo-VáZquez, D., Lorente-Plazas, R., Lorenzo-Lacruz, J., et al. (2013). The impact of the north atlantic oscillation on renewable energy resources in Southwestern Europe. *Journal of Applied Meteorology and Climatology*, *52*(10), 2204–2225. https://doi.org/10.1175/JAMC-D-12-0257.1

Jordahl, K., den Bossche, J., Van Fleischmann, M., Wasserman, J., McBride, J., Gerard, J., et al. (2019). geopandas/geopandas: V0.6.1. *Zenodo*. https://doi.org/10.5281/zenodo.3483425

Machowski, J., Lubosny, Z., Bialek, J. W., & Bumby, J. R. (2020). *Power system dynamics: Stability and control*. Wiley. Retrieved from https://books.google.ch/books?id=LZwmyAEACAAJ

Met Office. (2018). Cartopy: A cartographic python library with a Matplotlib interface. *Zenodo*. https://doi.org/10.5281/zenodo.1490296

Michelangeli, P. A., Vautard, R., & Legras, B. (1995). Weather regimes: Recurrence and quasi stationarity. *Journal of the Atmospheric Sciences*, *52*(8), 1237–1256. https://doi.org/10.1175/1520-0469(1995)052<1237:WRRAQS>2.0.CO;2

Pedregosa, F., Varoquaux, G., Gramfort, A., Michel, V., Thirion, B., Grisel, O., et al. (2011). Scikit-learn: Machine learning in Python. *Journal of Machine Learning Research*, *12*, 2825–2830.

Pfenninger, S., & Staffell, I. (2016). Long-term patterns of European PV output using 30 years of validated hourly reanalysis and satellite data. *Energy*, *114*, 1251–1265. https://doi.org/10.1016/j.energy.2016.08.060

Ram, M., Bogdanov, D., Aghahosseini, A., Oyewo, S., Gulagi, A., Child, M., & Breyer, C. (2017). *Global energy system based on 100% renewable energy – Power sector*. Study by Lappeenranta University of Technology and Energy Watch Group.

Rasmussen, M. G., Andresen, G. B., & Greiner, M. (2012). Storage and balancing synergies in a fully or highly renewable pan-European power system. *Energy Policy*, *51*, 642–651. https://doi.org/10.1016/j.enpol.2012.09.009

Schleussner, C. F., Rogelj, J., Schaeffer, M., Lissner, T., Licker, R., Fischer, E. M., et al. (2016). Science and policy characteristics of the Paris Agreement temperature goal. *Nature Climate Change*, *6*(9), 827–835. https://doi.org/10.1038/nclimate3096

SolarPower Europe and LUT University. (2020). 100% Renewable Europe – How to make Europe's energy system climate-neutral before 2050. Retrieved from https://api.solarpowereurope.org/uploads/Solar_Power_Europe_LUT_100_percent_Renewable_Europe_mr_804d34f698.pdf

Stram, B. N. (2016). Key challenges to expanding renewable energy. *Energy Policy*, *96*, 728–734. https://doi.org/10.1016/j.enpol.2016.05.034

Tröndle, T., Pfenninger, S., & Lilliestam, J. (2019). Home-made or imported: On the possibility for renewable electricity autarky on all scales in Europe. *Energy Strategy Reviews*, *26*(June), 100388. https://doi.org/10.1016/j.esr.2019.100388

van der Wiel, K., Bloomfield, H. C., Lee, R. W., Stoop, L. P., Blackport, R., Screen, J. A., & Selten, F. M. (2019). The influence of weather regimes on European renewable energy production and demand. *Environmental Research Letters*, *14*(9), 094010. https://doi.org/10.1088/1748-9326/ab38d3

Virtanen, P., Gommers, R., Oliphant, T. E., Haberland, M., Reddy, T., Cournapeau, D., et al. (2020). SciPy 1.0: Fundamental Algorithms for scientific computing in Python. *Nature Methods*, *17*(3), 261–272. https://doi.org/10.1038/s41592-019-0686-2

Wiese, F., Schlecht, I., Bunke, W. D., Gerbaulet, C., Hirth, L., Jahn, M., et al. (2019). Open power system data – Frictionless data for electricity system modelling. *Applied Energy*, *236*(June 2018), 401–409. https://doi.org/10.1016/j.apenergy.2018.11.097